Inorganic Chemistry

Article

pubs.acs.org/IC

$^2_\infty[Bi_2Cl_6(pyz)_4]$: A 2D-Pyrazine Coordination Polymer As Soft Host Lattice for the Luminescence of the Lanthanide Ions Sm^{3+}, Eu^{3+}, Tb^{3+}, and Dy^{3+}

Johanna Heine, Tobias Wehner, Rüdiger Bertermann, Andreas Steffen, and Klaus Müller-Buschbaum*

Institute of Inorganic Chemistry, Julius-Maximilians-University Würzburg, Am Hubland, 97074 Würzburg, Germany

Supporting Information

ABSTRACT: The 2D-coordination polymer $^2_\infty[Bi_2Cl_6(pyz)_4]$ was synthesized from $BiCl_3$ and a self-consuming melt of pyrazine (pyz). It proves to be a suitable soft host lattice for *in situ* co-doping of the lanthanide ions Sm^{3+}, Eu^{3+}, Tb^{3+}, and Dy^{3+} during network formation. The series of luminescent networks $^2_\infty[Bi_{(2-x)}Ln_xCl_6(pyz)_4]$ obtained exhibits an efficient antenna effect on the lanthanide ions. Emission is almost exclusively observed from the lanthanide centers at room temperature, whereas cooling to 77 K reveals a bismuth−pyrazine metal-to-ligand charge transfer related phosphorescence, which is also present without lanthanide participation. All parts of the coordination polymer can function for light uptake. Partial substitution is achieved by statistic replacement of bismuth with lanthanides and can range up to 25 at. % for trivalent europium.

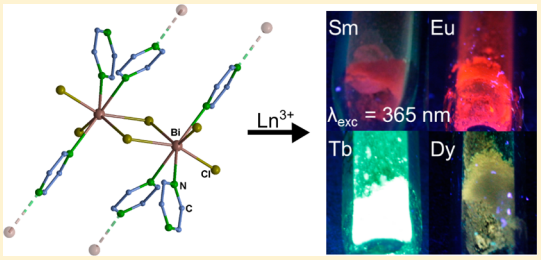

INTRODUCTION

Coordination polymers and the related metal−organic frameworks (MOFs) have been in the focus of research efforts during the past decade.[1] Their hybrid nature, composed of metal ions or clusters connected with organic linkers, gives rise to properties derived from either of the two or the combination of the components. The hybrid material can thereby generate cooperative properties, such as porosity,[2] magnetism,[3] photoluminescence,[4] or nonlinear optical properties.[5] Especially, photoluminescence is a prominent property that can be based on the organic ligands[6] or the metal centers.[7] Furthermore, energy transfers between ligand and metal ions can strongly support luminescence by the so-called antenna effect, in which the excited ligand transfers energy to the metal ions, followed by emission.[8] Lanthanide^{III} luminescence, stemming from 4f−4f transitions, has received attention in basic[9] and applied research[10] due to the highly predictable and line-like nature of these emissions, giving them a high color quality and covering a range from UV to IR. For many decades, lanthanide luminescence has mainly been studied either in solid-state phosphors or in complexes featuring chelating ligands that provide a defined coordination sphere free of quenching solvent molecules as well as π-systems for a sensitization of the lanthanide luminescence via an antenna effect.[8] This effect provides efficient means to circumvent the low absorption coefficients of the parity forbidden 4f−4f transitions: an allowed and thus intense absorption within a ligand molecule leads to an excited state whose energy is then transferred onto the lanthanide ion. More recently, inorganic−organic hybrid materials have come into the focus of lanthanide luminescence research, combining features from solid-state phosphors and molecular complexes.[11] Yet, while a great number of lanthanide coordination polymers and MOFs have been presented in the last years, containing potential luminescence centers as connectivity centers,[12] the solid-state technique of doping luminescence centers into a nonluminescent host lattice has received far less attention,[13] despite the potential to tune emission colors via co-doping of different luminescent ions[14] and to optimize quantum yields by avoiding concentration quenching effects.[15]

Bismuth-based coordination polymers and MOFs present attractive candidates for doping lanthanide ions into the lattice, since ionic radii and preferred coordination spheres of Bi^{3+} and trivalent lanthanide ions are similar. A few examples of lanthanide-doped bismuth-based coordination polymers and frameworks have been presented in recent years,[16] although all these interesting examples are based exclusively on carboxylate ligands. The chemistry of $BiCl_3$ and nitrogen donor ligands is still rather limited. Mainly, donor complexes involving ligands such as 2,2′-bipyridine or 1,10-phenanthroline have been explored,[17] but neutral coordination polymers involving $BiCl_3$ and nitrogen donors have not been reported up to now. The reason for this may to some extent lie in the water-sensitive nature of $BiCl_3$,[18] as a report by Morsali shows that the combination of $BiCl_3$ and 4,4′-bipyridine in methanol produces a salt-like compound consisting of partially protonated 4,4′-bipyridine and chlorobismuthate fragments. This appears to be the result of partial $BiCl_3$ hydrolysis to BiOCl and HCl.[19]

In this work, we present a coordination polymer built from $BiCl_3$ and pyrazine (pyz), obtained via a solvent-free synthesis route in a self-consuming melt of the ligand that avoids co-

Received: February 7, 2014
Published: June 25, 2014

   dx.doi.org/10.1021/ic500295r | Inorg. Chem. 2014, 53, 7197−7203

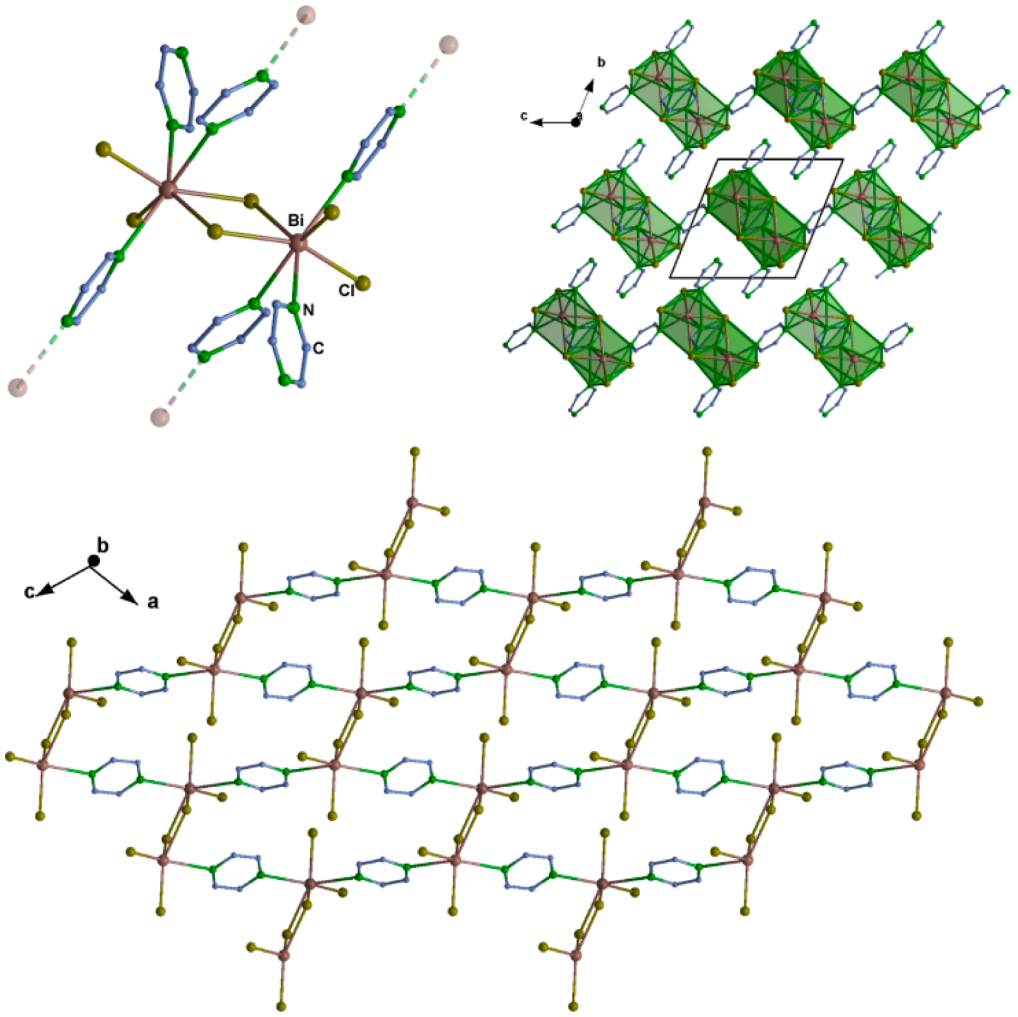

Figure 1. Excerpts of the crystal structure of $^{2}_{\infty}[Bi_2Cl_6(pyz)_4]$ (**1**). Main building unit (top left), polyhedral view along [100] (top right), and view along [010], with terminal pyrazine ligands omitted for clarity (bottom).

coordination of quenching solvent molecules or unwanted hydrolysis and instead yields the layered compound $^{2}_{\infty}[Bi_2Cl_6(pyz)_4]$ (**1**). We have studied the capability of this material to accept the luminescent lanthanide ions Sm^{3+}, Eu^{3+}, Tb^{3+}, and Dy^{3+}. Additionally, we have investigated the optical excitation and emission properties of the host lattice in detail. We thereby want to demonstrate the benefit of statistic replacement options of Bi^{III} in nitrogen-halide coordination with various trivalent lanthanide ions for luminescence and thus present a new bismuth-based coordination polymer as a soft host lattice for luminescence centers.

EXPERIMENTAL SECTION

General Data. All manipulations were carried out under inert atmospheric conditions using glovebox, ampule, and vacuum line techniques. Pyrazine (Acros, 99+%) and anhydrous $BiCl_3$ (Strem, 99.999%-Bi, PURATREM) were used as received. Anhydrous lanthanide trichlorides were prepared by the ammonium halide route[20] using the oxides Ln_2O_3 (ChemPur, 99.9%), HCl solution (10 mol/L, reagent grade), and ammonium chloride (Fluka, 99.5%) and purified by decomposition of the ternary trivalent ammonium chlorides under vacuum and subsequent sublimation of the products.

The microanalyses were carried out on a Vario Micro Cube analyzer.

^{13}C and ^{15}N VACP/MAS solid-state NMR spectroscopy was carried out on a Bruker DSX 400 NMR spectrometer using 4 mm ZrO_2 rotors containing ca. 50 mg of sample and a 4 mm MAS probe spinning the sample at a speed of 10 kHz. A 90° ^{1}H pulselength of 2.4 μs (^{13}C) or 2.7 μs (^{15}N) and a contact time of 2 ms (^{13}C) or 3 ms (^{15}N) were used. Compound **1** (bismuth only) was measured in the normal region of the expected chemical shifts (^{13}C: −50 to +250 ppm; ^{15}N: −400 to +50 ppm), while for compound **3** (2.0 at. % Eu^{3+}) the chemical shift range from −300 to 1250 ppm for ^{13}C was scanned.

The thermal investigation was carried out on **1** (36.1 mg) by simultaneous DTA/TG (Netzsch STA-409) in the temperature range of 25 to 900 °C with a heating rate of 10 °C min^{-1} in a constant flow of 20 mL min^{-1} Ar and 20 mL min^{-1} N_2.

For scanning electron microscopy (SEM) analysis, a SEM Zeiss ULTRA scanning electron microscope with a resolution of 1 nm at 15 kV was used. For imaging, different acceleration voltages between 2 and 20 kV together with an angle-selective backscattered electron (ASB) detector were used. This detector detects only the high-energy backscattered electrons, which are not or to a minor extent influenced by electrical charging effects. The energy-dispersive X-ray spectroscopy (EDX) analysis was performed using a Sapphire Si(Li) detector from EDAX at different acceleration voltages between 5 and 30 kV. Investigations were carried out exemplarily on a powdered sample of **4** (terbium co-doping). Samples were applied on an aluminum sample holder without any glue and rapidly transferred into the electron microscope. No sputtering was used, because the preparation had to be fast in order to avoid longer contact between the powder and air.

Photoluminescence excitation and emission spectra were recorded with a Horiba Jobin Yvon Fluorolog 3 photoluminescence spectrometer equipped with a 450 W Xe lamp, Czerny-Turner double

dx.doi.org/10.1021/ic500295r | Inorg. Chem. 2014, 53, 7197−7203

grating (1200 grooves per mm) excitation and emission monochromators, and an FL-1073 PMT detector. Excitation spectra were recorded from 250 to 600 nm and corrected for the spectral distribution of the lamp intensity using a photodiode reference detector. Emission spectra were recorded from 300 to 750 nm and corrected for the spherical response of the monochromators and the detector using typical correction spectra provided by the manufacturer. Additionally, the first and second harmonic oscillations of the excitation source were blocked by an edge filter (400 nm).

For some part of emission and excitation spectroscopy and the luminescence decay investigations, an Edinburgh Instruments FLSP920 spectrometer was used, equipped with double monochromators for the excitation and the emission paths, a red-sensitive PMT (R-928) operating at −20 °C, and a pulsed picosecond laser diode (375 nm, 5 mW), a microsecond flashlamp (μF920H, 100 W), and a 450 W Xe arc lamp as excitation sources. Luminescence decay time measurements were carried out in right-angle mode, and the obtained decays were corrected for the instrument response function. The investigations were carried out on **1** (bismuth only) as well as **3** (24.7 at. % of europium) under argon.

IR spectra were recorded with a Thermo Nicolet 380 FT-IR spectrometer in transmission mode; 5 mg of the compounds **1**−**5** were mixed with 300 mg of anhydrous KBr and pressed to transparent pellets.

X-ray Crystallography. Single-crystal X-ray determination was performed on crystals of $^{2}_{\infty}[Bi_2Cl_6(pyz)_4]$ (**1**) on a Bruker AXS Smart Apex 1 diffractometer with a graphite monochromator (Mo Kα radiation; λ = 0.710 73 Å) at a measurement temperature of 168 K. The structure was solved using direct methods, refined with ShelX,[21] and expanded using Fourier techniques, all within the OLEX2 software suite.[22] All non-hydrogen atoms were refined anisotropically. Hydrogen atoms were assigned to idealized geometric positions and included in structure factor calculations.

Powder patterns of **1** and the co-doped compounds **2**−**5** were recorded on STOE STADI P Debye−Scherrer X-ray diffractometers with Mo Kα_1 radiation with λ = 0.709 30 Å. Samples were prepared in a sealed glass capillary with a diameter of 0.2 mm.

Synthesis of $^{2}_{\infty}[Bi_2Cl_6(pyz)_4]$ (1). A mixture of pyrazine (101.1 mg, 1.25 mmol) and $BiCl_3$ (78.8 mg, 0.25 mmol) was transferred into a Duran glass ampule. The ampule with the reaction mixture was cooled to 77 K in liquid nitrogen to avoid sublimation of pyrazine, evacuated, and sealed under vacuum. The mixture was heated in an alumina tube oven with digital thermo control to 50 °C in 4 h, held at that temperature for 72 h, heated to 70 °C in 24 h, held for 48 h, cooled to 50 °C in 24 h, and finally cooled to room temperature in 4 h. After the reaction, excess pyrazine was removed by sublimation at 50 °C, and **1** was obtained as a crystalline, colorless powder.

Data for **1**: Anal. Calcd for $Bi_2Cl_6N_8C_{16}H_{16}$ (M = 951.03 g mol^{-1}): C, 20.21; H, 1.70; N, 11.78. Found: C, 19.62; H, 1.70; N, 11.19. MIR (KBr) in cm^{-1}: 3475 w, 3097 w, 3029 w, 1636 w, 1414 vs, 1155 m, 1121 s, 1039 s, 806 w, 794 m, 439 m, 419 w. ^{13}C solid-state NMR: 147.8 and 145.0 ppm.

Synthesis of Lanthanide-Doped Samples $[Bi_{(2-x)}Ln_xCl_6(pyrazine)_4]$ (2−5). The reaction mixture was prepared and treated as described above with the respective lanthanide trichloride replacing some part x of the amount of $BiCl_3$ by $LnCl_3$. To ensure sample homogeneity, the mixture was thoroughly ground before heating. For samarium (**2**) 5.6 at. % of $SmCl_3$ was added (x = 0.12), for europium (**3**) 2.0 at. % (x = 0.04), 3.2 at. % (x = 0.06), 19.0 at. % (x = 0.38), and 24.7 at. % (x = 0.49) of $EuCl_3$ were used, for terbium (**4**) 4.6 at. % (x = 0.09), 9.1 at. % (x = 0.18), and 20.8 at. % (x = 0.42) of $TbCl_3$ were used, and for dysprosium (**5**) 4.6 at. % (x = 0.09) of $DyCl_3$ was included. Phase purity was confirmed via a PXRD measurement (see Figure 4) and lanthanide incorporation/doping via the respective luminescence spectra (see Figures 6, 7, and S3−S9).

Reaction yields for **2**−**5** were 202 to 215 mg (85−90% with respect to the metal chloride).

^{13}C solid-state NMR (**3**, 2.0-at. % Eu^{3+}): 147.9, 145.1 ppm.

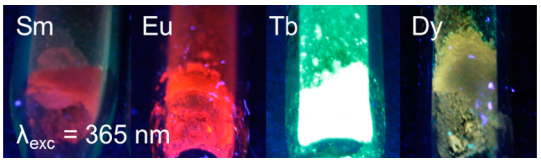

Figure 2. Emission colors of lanthanide-doped networks $^{2}_{\infty}[Bi_{(2-x)}Ln_xCl_6(pyz)_4]$ (Sm: **2**, Eu: **3**, Tb: **4**, Dy: **5**).

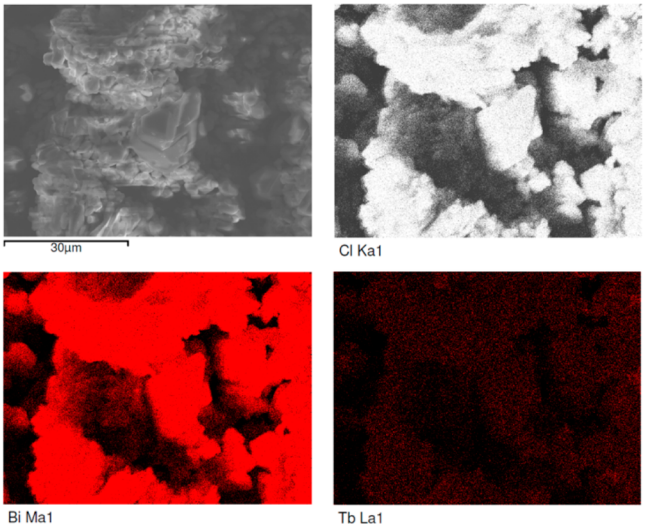

Figure 3. SEM image (top left) and EDX mappings of $^{2}_{\infty}[Bi_{(2-x)}Tb_xCl_6(pyz)_4]$ (**4**), x = 0.09.

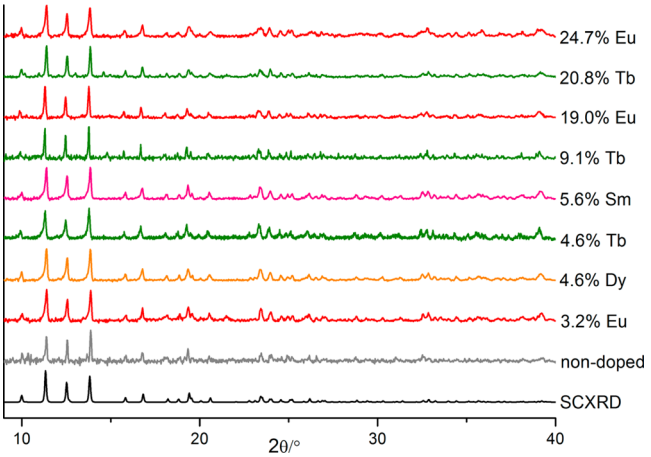

Figure 4. Powder diffraction patterns of **1** and co-doped **2**−**5** (Sm: **2**, Eu: **3**, Tb: **4**, Dy: **5**) with different lanthanide contents and the pattern simulated from single-crystal data of **1**.

DISCUSSION

Reaction of $BiCl_3$ in molten pyrazine at 70 °C and subsequent removal of excess pyrazine by sublimation yields colorless plate-like crystals of $^{2}_{\infty}[Bi_2Cl_6(pyz)_4]$ (**1**). The crystal structure analysis reveals a layered 2D structure with a honeycomb-like topology for **1**, giving a rare example of a bismuth-N-donor interlinked network. The main building unit consists of Bi_2Cl_6 dimers with two bridging and one terminal pyrazine ligand per Bi atom. Bismuth atoms, which occupy only one crystallographic site, are 7-fold coordinated by three nitrogen and four chlorine atoms, forming a capped trigonal prismatic coordination polyhedron (Figure 1).

dx.doi.org/10.1021/ic500295r | Inorg. Chem. 2014, 53, 7197−7203

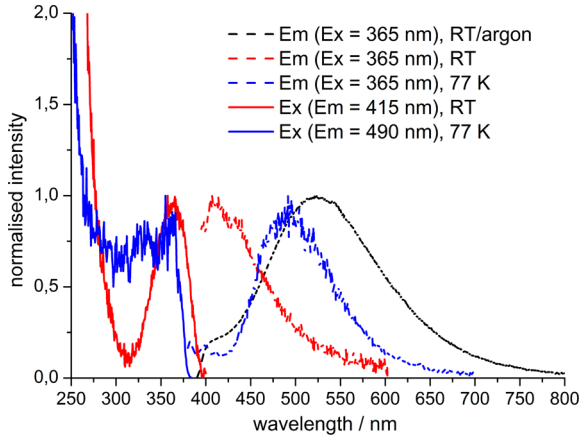

Figure 5. Excitation (normalized to the maximum signal of the lowest energy transition) and emission spectra (normalized to the respective maximum) of **1** at room temperature and 77 K.

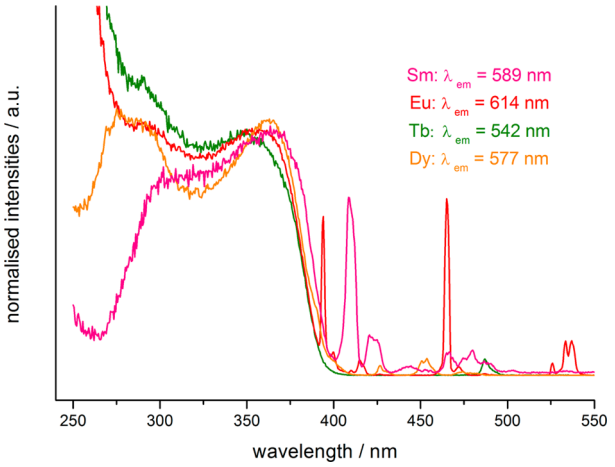

Figure 7. Normalized excitation spectra of **2**–**5** (lanthanide contents: Sm: 5.6%; Eu: 3.2%; Tb: 4.6%; Dy: 4.6%) recorded at room temperature. The emission wavelengths chosen correspond to the strongest emission bands for all cases. See Supporting Information for a detailed view and assignment of the f–f transitions.

In line with its usually predominant spherical 6s character, the lone pair of the Bi^{3+} ions is not stereoactive in this compound. The Bi–N-distances range from 249.1(6) to 275.0(7) pm. This accords well with the distances found in bismuth halide donor complexes such as $Bi_2Cl_6(2,2\text{-bipy})_3$, in which Bi–N distances range from 252 to 271 pm.[17] The wide range of Bi–N distances observed in **1** is caused by the two different pyrazine coordination modes, bridging and terminal, with larger distances observed for bridging ligands. The Bi–Cl

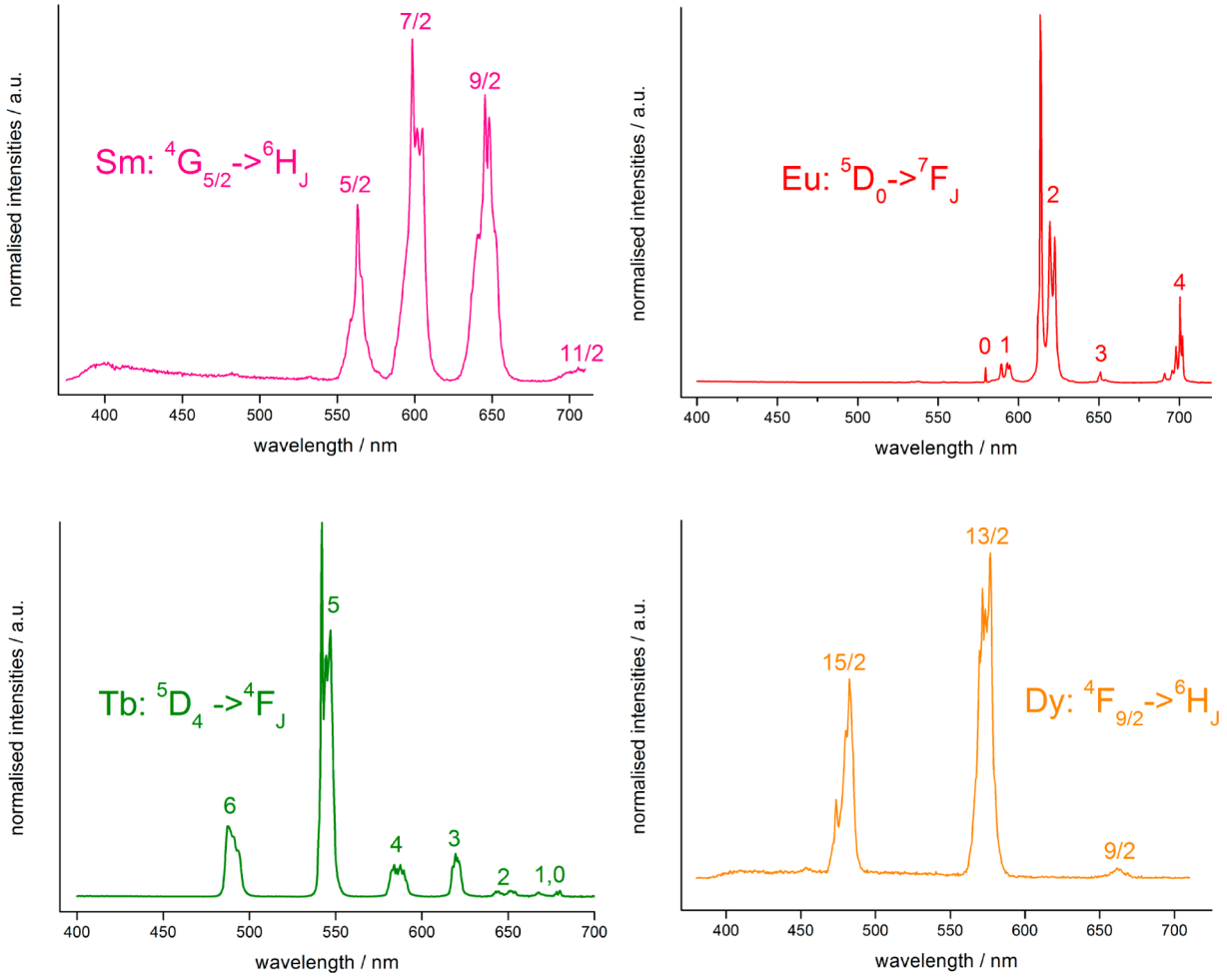

Figure 6. Normalized emission spectra of **2**–**5** (lanthanide contents: Sm: 5.6%; Eu: 3.2%; Tb: 4.6%; Dy: 4.6%) recorded at room temperature. The excitation wavelength is 365 nm for **2**–**5**.

dx.doi.org/10.1021/ic500295r | Inorg. Chem. 2014, 53, 7197–7203

distances are in the range of 256.3(2) to 305.37(17) pm, similar to literature examples such as [(mes-BIAN)$BiCl_3$] (mes-BIAN = 1,2-bis(mesitylimino)acenaphthene), where Bi−Cl distances of 250 to 305 pm are found.[23] Like the Bi−N distances, the Bi−Cl distances are also significantly influenced by the coordination mode of the chloride ligand, again with larger distances observed for the symmetrically bridging anions.

In order to achieve luminescence, doping is carried out during synthesis by adding appropriate amounts of $LnCl_3$ (Ln = Sm, Eu, Tb, Dy), resulting in compounds of the composition $^2_\infty[Bi_{(2-x)}Ln_xCl_6(pyz)_4]$ (Sm: **2**, Eu: **3**, Tb: **4**, Dy: **5**). The doped materials display the characteristic luminescence colors and fingerprint spectra of the respective lanthanides, as shown in Figure 2.

In principle, doping of a host lattice with other metal ions during synthesis can lead to either a statistic replacement of the different metals, a new bimetallic phase being formed, or, in case both components do not mix, phase separation of the two products. Especially, low concentrations of dopants make it difficult to identify the character of the products. When doping a coordination polymer as a soft host lattice with an ion that is not an exact fit with regard to size, charge, and chemical behavior, it is a challenge to prove that an actual statistic replacement of the host lattice ions with the dopant has occurred instead of the formation of a well-dispersed minor separate phase composed of a different coordination polymer built from the dopant and the ligands used during synthesis. We have set out to prove that actual doping has occurred in our compound series **2**−**5** by employing a number of different methods: A first indication that doping and not phase separation has occurred is provided by elemental mapping with EDX measurements. An exemplary investigation of **4** with a terbium content of 4.5% is shown in Figure 3. The elemental mapping shows a homogeneous dispersion of terbium on a submicrometer level, and the 5-nm-resolved point EDX analysis accords well with the expected terbium content based on a Bi/Tb ratio of 1.91:0.09.

X-ray powder diffraction is a reliable tool to provide information about different phases contained within bulk materials. Yet, when investigating doped materials, the limit of detection of this method can hinder identification of minority phases. Secondary phases that make up less than 5% of the bulk material are usually difficult, if not impossible, to detect by X-ray sources. This is also the case for small amounts of amorphous phases.

Therefore, also ^{13}C and ^{15}N VACP/MAS solid-state NMR spectroscopy were carried out on $^2_\infty[Bi_2Cl_6(pyz)_4]$ (**1**) and despite potential problems due to paramagnetism on $^2_\infty[Bi_{(2-x)}Eu_xCl_6(pyz)_4]$ (**3**), x = 0.04. For ^{13}C NMR both samples show only two signals at about 148 and 145 ppm, expected for the two different carbon atoms in the pyrazine ligand.[24] The identical chemical shift and line width in the ^{13}C NMR spectra indicate the chemical identity of both samples and the absence of any additional observable phase. However, compound **3** was investigated for further ^{13}C signals in the range from −300 to 1250 ppm, but no additional signals could be detected. This corroborates the findings of PXRD, elemental analyses, and luminescence decay, thereby supporting statistic metal replacement. However, the detection limits of the method (VACP/MAS) also have to be considered: a low amount of carbons neighboring Eu^{3+} (x = 0.04) with a lack of visibility by paramagnetic line broadening and failure of the cross-polarization due to too quick relaxation of the carbon atoms caused by the paramagnetic moment of the neighboring europium ion. It is hence remarkable that the paramagnetic sample **3** gives a reasonable spectrum at a much shorter measurement time than the diamagnetic bismuth compound **1** (Figure S11). The low amount of paramagnetic Eu^{3+} ions obviously has no negative but a rather beneficial influence on ^{13}C NMR, whereas the quadrupole moment of Bi^{3+} (^{209}Bi: I = 9/2, Q = −51.6 fm^2, 100%) has a nonpositive influence, as no ^{15}N NMR signals for both samples could be detected in the ^{15}N VACP/MAS solid-state NMR spectra.

In addition, we have also prepared samples with high lanthanide contents to test the limits of acceptance of the host lattice. Europium- and terbium-doped samples provide an interesting example of this approach, while europium-doped samples show no secondary phase formation even at 25% europium content of **3**. Acceptance of the smaller terbium ions in **4** appears much lower, and secondary phase formation starts to become evident at 10% terbium content. The reason for this may lie in the slightly smaller ionic radius of Tb^{3+} compared to Eu^{3+} (effective ionic radii for coordination number 6: Dy^{3+} 91.2 pm, Tb^{3+} 92.3 pm, Eu^{3+} 94.7 pm, Sm^{3+} 95.8 pm, Bi^{3+} 103 pm),[25] giving a better fit for Eu^{3+}. An overview of the recorded powder patterns is given in Figure 4. It shows that all powder patterns are identical for the dopant degrees chosen and that lanthanide ions can fairly well substitute bismuth in the trivalent state, except for the largest amounts of Tb^{3+}, for which small additional reflection intensities can be observed (see also Figure S2). The secondary phase formed in the Tb-doped samples does not match any of the starting materials and appears for Tb contents of 10% or more. The secondary phase possibly consists of either a heterometallic Bi−Tb compound or a pure $TbCl_3(pyz)_n$ coordination polymer. Unfortunately, such compounds have not yet been reported; accordingly, no comparison is available. This finding shows that the host lattice cannot accept larger amounts of Tb^{3+} ions on one hand; it also serves to prove that a phase separation in the system $BiCl_3$/$LnCl_3$/pyrazine can be deduced from PXRD measurements. Thus, there is further evidence that the highly europium doped samples contain no observable secondary phase but only one single product.

For a discussion of the luminescence properties of co-doped lanthanide ions within the host lattice $^2_\infty[Bi_2Cl_6(pyz)_4]$ (**1**), we have studied the excitation and emission spectra of the nondoped material. These are shown in Figure 5. The excitation spectra at room temperature and 77 K show a maximum at 365 nm as well as its intensity maximum at λ < 250 nm ranging up to 300 nm. At room temperature, the emission spectrum shows a weak and broad emission band at 405 nm. To the naked eye the nondoped material is nonluminescent at room temperature. However, when we prepared a second sample for the luminescence measurements under rigorous exclusion of air by the use of screw-capped cuvettes under strict inert argon conditions, in addition to the weak emission at 405 nm, a second, more intense emission band with a maximum at λ_{max} = 520 nm was detected. At 77 K the emission spectrum again shows the broad band at 495 nm, resulting in a weak, but visible bluish-white luminescence. We assign the high-energy emission as residual fluorescence, which appears to be quenched by intersystem crossing to a triplet state, leading to low-energy phosphorescence. It is feasible that the emission band at 520 nm can be quenched by traces of oxygen (*vide supra*), as is typical for phosphorescence, consequently showing only the fluorescence band. This

dx.doi.org/10.1021/ic500295r | Inorg. Chem. 2014, 53, 7197−7203

conclusion is also supported by our lifetime investigations of the luminescence decay (*vide infra*).

The precise assignment of electronic transitions in bismuth coordination polymers is notoriously difficult, since a number of different transitions are possible: pure ligand-based n−π^* and π−π^* transitions, as well as charge transfer processes, being either metal-to-ligand charge transfer (MLCT) from Bi^{3+} to an electron-poor ligand or ligand-to-metal-charge transfer (LMCT) from an electron-rich ligand to Bi^{3+}. Additionally, Bi^{3+} can undergo metal-centered s → p transitions. These mechanisms are available for absorption as well as emission and have all been previously observed for different bismuth-containing systems.[26] A comparison of the excitation and emission spectra of **1** with those of pure crystalline pyrazine (see Figures S7 and S8) shows that, while ligand-based transitions may certainly play a role in absorption processes between 250 and 330 nm, absorption at 350 nm and higher as well as the significant emission band at 520 nm recorded at room temperature and 495 nm at 77 K cannot be explained solely based on pure ligand transitions. Comparison with the absorption spectra of a series of donor complexes [M(2,2′-bipyridyl)X_3], with M = Sb, Bi and X = Cl, Br, I,[26d] suggests an MLCT mechanism from Bi^{3+} to the pyrazine ligand for the absorption band at 365 nm.

The room-temperature excitation and emission spectra of the doped materials $^2_\infty[Bi_{(2-x)}Ln_xCl_6(pyz)_4]$ (Sm: **2**, Eu: **3**, Tb: **4**, Dy: **5**) are summarized in Figures 6 and 7 (see Supporting Information for spectra of **3** and **4** at 77 K and separate excitation and emission spectra of **2** and **5**, Figures S3−S6). The excitation spectra are similar to the nondoped material, but additionally show direct 4f−4f transitions as sharp excitation lines. This indicates that an energy transfer from excited bismuth-based MLCT states is possible, giving further evidence that lanthanide ions are located within the host lattice and not in a secondary phase. The emission spectra display typical 4f−4f emissions. At room temperature, these are strong compared to the high-energy luminescence of the host lattice at 405 nm, while the phosphorescence at 520 nm is nearly completely quenched. This indicates either energy transfer from this triplet excited state to the lanthanides or an additional nonradiative pathway introduced by the co-doping with lanthanides. Interestingly, at 77 K the host-based luminescence becomes more significant. Antenna effects for lanthanide luminescence are typically based on excited ligand states. Antenna effects based on the excited charge transfer states of metal complexes offer the advantage of absorption bands that are usually lower in energy than ligand transitions.[27] This is also the case for our material, for which ligand transitions are located at shorter wavelengths, while a strong MLCT excitation band is observed close to the visible range.

Europium luminescence provides additional information on the coordination environment of Eu^{3+} [28] (see Supporting Information for a detailed view of the emissions in **3** at 77 K, Figure S3). The presence of the $^5D_0 \rightarrow {}^7F_0$ transition, the fine structure of the $^5D_0 \rightarrow {}^7F_{1-4}$ transitions, and a large value of the intensity ratio $R = I(^5D_0 \rightarrow {}^7F_2)/I(^5D_0 \rightarrow {}^7F_1)$ are consistent with the low-symmetry coordination environment of Bi^{3+} found in **1**. Thus, this is an additional indication that the Ln^{3+} ions statistically replace Bi^{3+} in the coordination polymer and that a truly doped material is obtained from this synthesis route.

For further insights, the luminescence lifetimes were studied on the bismuth-only compound **1** as well as on the highest homogeneous Eu content (**3**) of 24 at. %. The residual emission at 405 nm of $^2_\infty[Bi_2Cl_6(pyz)_4]$ (**1**) was too weak to be determined by decay investigations. However, although the luminescence decay of the emission band at λ_{max} = 520 nm is too weak to be measured with our pulsed laser diode (see Experimental Section) at a repetition rate of 5 μs, it appears to be shorter than the spectroscopic resolution of the instrument when excited with a 60 W xenon microsecond flashlamp (10 μs). This leads us to conclude that the emission is phosphorescent in nature, and although we were not able to determine the lifetime accurately, it must be in the range of a few microseconds. The europium-doped compound **3** exhibits a much longer luminescence lifetime. A biexponential decay is observed upon excitation at λ = 365 nm, giving values of 547(12) and 723(26) μs for the emission $^5D_0 \rightarrow {}^7F_2$ and 584(7) and 936(101) μs for $^5D_0 \rightarrow {}^7F_4$ of Eu^{3+}. Due to the fact that at a wavelength of 365 nm no direct Eu^{3+} excitation can occur, but excitation at that energy allows light uptake via the other framework components, the decay investigation also supports the antenna effect by the MLCT excitation identified in the photoluminescence spectra and thus bismuth participation in the luminescence process of the lanthanide containing networks.

Finally, the thermal behavior of **1** (36.1 mg) was studied by simultaneous DTA/TG (Netzsch STA-409) from 25 to 900 °C with a heating rate of 10 °C min^{-1} in a constant flow of 20 mL min^{-1} Ar and 20 mL min^{-1} N_2 (see Figure S9). Three mass loss steps are detected. While the first mass loss at 120 °C of 7% accords well with the loss of one pyrazine molecule per formula unit, the subsequent steps cannot be easily identified and are likely to be a combination of pyrazine loss, decomposition, and the onset of $BiCl_3$ sublimation above 300 °C.

CONCLUSION

To summarize, the solvent-free reaction of $BiCl_3$ with a melt of pyrazine gave the two-dimensional coordination polymer $^2_\infty[Bi_2Cl_6(pyz)_4]$ (**1**), which proves to be a suitable host lattice for co-doping with the lanthanide ions Sm^{3+}, Eu^{3+}, Tb^{3+}, and Dy^{3+}. Statistic replacement of bismuth and the lanthanide ions yields the luminescent compounds $^2_\infty[Bi_{(2-x)}Ln_xCl_6(pyz)_4]$ (**2**−**5**, Ln = Sm, Eu, Tb, Dy), corroborated by PXRD, elemental analysis, solid-state ^{13}C NMR, photoluminescence spectroscopy, and luminescence decay investigations. The range of homogeneous co-doping varies depending on the lanthanide. Acceptance of lanthanide ions ranges up to 25% for Eu^{3+}, whereas Tb^{3+} shows side phase formation already for 10% terbium. The four trivalent lanthanide ions chosen in principle illustrate that bismuth is a suitable center for substitution with lanthanides by means of size, charge, and chemical surrounding, especially as it is non-stereoactive. The photoluminescence of the co-doped networks is triggered by ligand-based temperature-dependent excitation between 250 and 330 nm, as well as bismuth- and lanthanide-based excitation at λ > 350 nm. Energy can be transferred from the ligand to bismuth and to the lanthanide ions, giving the most intense emission for Eu^{3+} and Tb^{3+}. The energy transfer is efficient, as no other emissions are observed except by 4f−4f transitions and a very weak remaining pyrazine emission around 400 nm. The latter proves also to be temperature dependent for the nondoped compound **1**, being more pronounced at 77 K. To the best of our knowledge, this series of compounds marks the first examples of lanthanide co-doped bismuth coordination polymers that are not carboxylates. They further illustrate the value of nitrogen-donor and

dx.doi.org/10.1021/ic500295r | Inorg. Chem. 2014, 53, 7197−7203

halide ligands as efficient antenna for luminescence of trivalent lanthanide ions together with Bi^{3+}.

■ ASSOCIATED CONTENT

Supporting Information

Crystallographic details, additional PL spectra, thermogravimetric analysis. Cif for CCDC-977661. This material is available free of charge via the Internet at http://pubs.acs.org.

■ AUTHOR INFORMATION

Corresponding Author

*E-mail: k.mueller-buschbaum@uni-wuerzburg.de. Fax: +49-931-3184785. Tel: +49-931-3188724.

Notes

The authors declare no competing financial interest.

■ ACKNOWLEDGMENTS

The authors gratefully acknowledge the Deutsche Forschungsgemeinschaft (DFG) and the Program for Equal Chances for Women in Science and Research of the State of Bavaria.

■ REFERENCES

(1) Janiak, Ch.; Vieth, J. K. *New J. Chem.* **2010**, *34*, 2366−2388.
(2) Kitagawa, S.; Kitaura, R.; Noro, S.-i. *Angew. Chem.* **2004**, *116*, 2388−2430; *Angew. Chem., Int. Ed.* **2004**, *43*, 2334−2375.
(3) Coronado, E.; Espallargas, G. M. *Chem. Soc. Rev.* **2013**, *42*, 1525−1539.
(4) Allendorf, M. D.; Bauer, C. A.; Bhakta, R. K.; Houk, R. J. T. *Chem. Soc. Rev.* **2009**, *38*, 1330−1352.
(5) Cui, Y.; Yue, Y.; Qian, G.; Chen, B. *Chem. Rev.* **2012**, *112*, 1126−1162.
(6) Almeida Paz, F. A.; Klinowski, J.; Vilela, S. M. F.; Tomé, J. P. C.; Cavaleiro, J. A. S.; J. Rocha, J. *Chem. Soc. Rev.* **2012**, *41*, 1088−1110.
(7) Heine, J.; Müller-Buschbaum, K. *Chem. Soc. Rev.* **2013**, *42*, 9232−9242.
(8) Armelaoa, L.; Quicib, S.; Barigelletti, F.; Accorsi, G.; Bottaro, G.; Cavazzini, M.; Tondello, E. *Coord. Chem. Rev.* **2010**, *254*, 487−505.
(9) Bünzli, J.-C. G.; Eliseeva, S. V. In *Springer Series on Fluorescence, Vol. 7, Lanthanide Spectroscopy, Materials, and Bio-applications*; Springer Verlag: Berlin, 2010; Chapter 2.
(10) Bünzli, J.-C. G.; Eliseeva, S. V. *Chem. Sci.* **2013**, *4*, 1939−1949.
(11) Binnemans, K. *Chem. Rev.* **2009**, *109*, 4283−4374.
(12) Rocha, J.; Carlos, L. D.; Almeida Paz, F. A.; Ananias, D. *Chem. Soc. Rev.* **2011**, *40*, 926−940.
(13) (a) Serre, C.; Millange, F.; Thouvenot, C.; Gardant, N.; Pellé, F.; Férey, G. *J. Mater. Chem.* **2004**, *14*, 1540−1543. (b) Bo, Q.-B.; Wang, H.-Y.; Wang, D.-Q.; Zhang, Z.-W.; Miao, J.-L.; Sun, G.-X. *Inorg. Chem.* **2011**, *50*, 10163−10177. (c) Sava, D. F.; Rohwer, L. E. S.; Rodriguez, M. A.; Nenoff, T. M. *J. Am. Chem. Soc.* **2012**, *134*, 3983−3986. (d) Depending on the specific area of chemistry or material science in question, the term doping can cover dopant concentrations from ppb to the percent range. In this article, we use the term to emphasize that a statistical replacement occurred, not in the sense that only ppm or ppb amounts of dopant have been used..
(14) Matthes, P. R.; Höller, C. J.; Mai, M.; Heck, J.; Sedlmaier, S. J.; Schmiechen, S.; Feldmann, C.; Schnick, W.; Müller-Buschbaum, K. *J. Mater. Chem.* **2012**, *22*, 10179−10187.
(15) Zurawski, A.; Mai, M.; Baumann, D.; Feldmann, C.; Müller-Buschbaum, K. *Chem. Commun.* **2011**, *47*, 496−498.
(16) (a) Thirumurugan, A.; Tan, J.-C.; Cheetham, A. K. *Cryst. Growth Des.* **2010**, *10*, 1736−1741. (b) Thirumurugan, A.; Cheetham, A. K. *Eur. J. Inorg. Chem.* **2010**, 3823−3828. (c) Thirumurugan, A.; Li, W.; Cheetham, A. K. *Dalton Trans.* **2012**, *41*, 4126−4134. (d) Zhang, X.-P.; Wang, D.-G.; Su, Y.; Tian, H.-R.; Lin, J.-J.; Feng, Y.-L.; Cheng, J.-W. *Dalton Trans.* **2013**, *42*, 10384−10387. (e) Feyand, M.; Köppen, M.; Friedrichs, G.; Stock, N. *Chem.—Eur. J.* **2013**, *19*, 12537−1254.
(17) (a) Bowmaker, G. A.; Hannaway, F. M. M.; Junk, P. C.; Lee, A. M.; Skelton, B. W.; White, A. H. *Aust. J. Chem.* **1998**, *51*, 317−324. (b) Bowmaker, G. A.; Hannaway, F. M. M.; Junk, P. C.; Lee, A. M.; Skelton, B. W.; White, A. H. *Aust. J. Chem.* **1998**, *51*, 325−330. (c) Bowmaker, G. A.; Hannaway, F. M. M.; Junk, P. C.; Lee, A. M.; Skelton, B. W.; White, A. H. *Aust. J. Chem.* **1998**, *51*, 331−336.
(18) Wosylus, A.; Hoffmann, S.; Schmidt, M.; Ruck, M. *Eur. J. Inorg. Chem.* **2010**, 1469−1471.
(19) Soltanzadeh, N.; Morsali, A. *Polyhedron* **2009**, *28*, 1343−1347.
(20) Meyer, G. *Inorg. Synth.* **1989**, *25*, 146−150.
(21) Sheldrick, G. *Acta Crystallogr.* **2008**, *A64*, 112−122.
(22) Dolomanov, O. V.; Bourhis, L. J.; Gildea, R. J.; Howard, J. A. K.; Puschmann, H. *J. Appl. Crystallogr.* **2009**, *42*, 339−341.
(23) Hill, N. J.; Reeske, G.; Moore, J. A.; Cowley, A. H. *Dalton Trans.* **2006**, 4838−4844.
(24) Kalinowski, H.-O.; Berger, S.; Braun, S. In *^{13}C-NMR-Spektroskopie*; Georg Thieme Verlag: Stuttgart, 1984; p 351.
(25) Shannon, R. D. *Acta Crystallogr.* **1976**, *A32*, 751−767.
(26) (a) Wibowo, A. C.; Smith, M. D.; zur Loye, H.-C. *Chem. Commun.* **2011**, *47*, 7371−7373. (b) Mason, W. R. *Inorg. Chem.* **1999**, *38*, 2742−2745. (c) Nikol, H.; Vogler, A. *J. Am. Chem. Soc.* **1991**, *113*, 8988−8990. (d) Kunkely, H.; Paukner, A.; Vogler, A. *Polyhedron* **1989**, *8*, 2937−2939.
(27) Ward, M. D. *Coord. Chem. Rev.* **2007**, *251*, 1663−1677.
(28) Tanner, P. A. *Chem. Soc. Rev.* **2013**, *42*, 5090−5101.